Nitrate drawdown during a shelf sea spring bloom revealed using a novel microfluidic *in situ* chemical sensor deployed within an autonomous underwater glider

Alexander G. Vincent[1]*, Robin W. Pascal[2], Alexander D. Beaton[2], John Walk[2], Joanne E. Hopkins[3], E. Malcolm S. Woodward[4], Matthew Mowlem[2], Maeve C. Lohan[1].

1. Ocean and Earth Science, University of Southampton, Southampton, SO14 3ZH, UK

2. Ocean Technology and Engineering Group, National Oceanography Centre, Southampton, SO14 3ZH, UK

3. National Oceanography Centre, Joseph Proudman Building, Liverpool, L3 5DA, UK

4. Plymouth Marine Laboratory, Prospect Place, Plymouth, PL1. 3DH, UK

* Corresponding author at: Ocean and Earth Science, National Oceanography Centre Southampton, SO14 3ZH, UK.

Email address: agv1e15@soton.ac.uk

Keywords: Microfluidics; Autonomous Underwater Vehicles; Shelf Seas; Nutrients

Abstract

Here we describe, for the first time, the use of a miniaturized Lab-on-Chip (LoC) nutrient sensor deployed within an autonomous underwater vehicle (AUV; Kongsberg Seaglider) to collect high-resolution nitrate (nitrate + nitrite) data in a highly dynamic shelf sea environment. Seasonally stratified temperate shelf seas act as important carbon sinks, where primary production is controlled by the availability of nutrients such as nitrate. Spring phytoplankton blooms and sporadic mixing events can drastically modify the availability of nitrate on temporal scales from hours to days.

Traditional sampling methods are unable to capture high frequency events that can be clearly observed using a wet-chemical microfluidic system deployed within a glider. We highlight firstly, an excellent agreement between the LoC and shipboard nitrate + nitrite measurements (r^2 = 0.98 n = 11) during the onset of a spring bloom. Secondly, the LoC was able to observe a decrease in nitrate within the surface mixed layer from 5.74 µM (4th) to 1.42 µM (25th), whilst bottom layer$^-$ concentrations remained constant (6.86 ± 0.16 µM), with an estimated analytical uncertaintly of < 0.2 µM. Thirdly, the ability of an LoC sensor deployed within an AUV to accurately capture simultaneous biogeochemical and physical parameters at an enhanced resolution, on both spatial and temporal scales, improves our understanding of biogeochemical cycles within the dynamic temperate shelf sea environments.

1. Introduction

Seasonally stratified, temperate shelf seas act as important global carbon sinks through the continental shelf pump mechanism (Tsunogai, Watanabe and Sato, 1999; Thomas *et al.*, 2004; Takahashi *et al.*, 2009). Despite the shelf seas' relatively small size (8% of global ocean area), they actually account for 15–30% of total oceanic primary production (Tweddle *et al.*, 2013) and have an average carbon fixation rate per unit area ~2.5 times greater than the open ocean (Simpson and Sharples, 2012). The interplay between light, nutrients and mixing are key drivers of primary production. A well-studied temperate shelf system, the Celtic Sea, shows a clear seasonal cycle whereby initial light and nutrient conditions are ideally suited to support the onset of the spring bloom (Fasham, Holligan and Pugh, 1983). This results in the rapid drawdown of nitrate (NO_3^-) from ~ 6-8 µM to below the limit of detection (<0.1 µM) (e.g. Hickman *et al.*, 2012; Davidson *et al.*, 2013). Post-bloom, new primary production is limited to the sub-

surface chlorophyll maximum (SCM) where fluxes of NO_3^- into the thermocline fuels new production (Hickman *et al.*, 2009).

In the central Celtic Sea, shear generated turbulence (Sharples *et al.*, 2001, 2007; Rippeth *et al.*, 2009) and wind-driven oscillations (Tom P. Rippeth, 2005) are the central mechanisms in driving diapycnal mixing of NO_3^- up into the nutrient deplete surface mixed layer. Wind-driven shear occurs in episodic short-lived spikes (0.5-1 hr) and has the potential to have a large impact on NO_3^- fluxes, with observations indicating that this flux can be up to 4 times greater than when no shear was observed (Sharples *et al.*, 2001; Palmer, Rippeth and Simpson, 2008; Rippeth *et al.*, 2009).

At present, it is difficult to effectively sample nitrate at the high resolution required to observe these key short-term mixing events (Sharples *et al.*, 2007; Charlotte Williams *et al.*, 2013). Combined with limited winter data, this can lead to incorrect seasonal estimates of NO_3^- fluxes that are key to primary production and carbon fixation. Chemical *in-situ* sensors can provide high-resolution data necessary to resolve biogeochemical processes occurring in shelf seas (Prien, 2007; Adornato *et al.*, 2010). Wet-chemical analysers, centred on microfluidic Lab-on-Chip (LoC) technology, are at the leading edge of advancements for chemical *in-situ* nutrient measurements (Nightingale, Beaton and Mowlem, 2015). Due to their compactness, low resource use and analytical performance comparable to laboratory-based methods, LoC nutrient sensors are well suited to high-resolution float, glider and mooring deployments. Autonomous underwater vehicles, such as gliders, have already been shown to provide an economic and efficient observation platform to resolve mesoscale and submesoscale structures, allowing for high-resolution sampling of biogeochemical parameters, such as NO_3^- using an *in situ* ultraviolet spectrophotometer (Johnson *et al.*, 2009,2017; Rudnick, 2016).

Here we demonstrate the power of coupling the LoC nutrient sensor into a Seaglider to obtain continuous *in-situ* high temporal and spatial resolution nitrite + nitrate (NO_3^- +NO_2^-, hereafter defined as $\sum NO_x$) measurements over the duration of the spring bloom in April 2015. This enabled short-term mixing events key to establishing the spring bloom and its subsequent decline to be observed.

2. Experimental

A single LoC ΣNO_x sensor (Ocean Technology and Engineering Group, National Oceanography Center, Southampton, UK) was integrated within the science bay of a Kongsberg Seaglider (Ogive fairing) and deployed from the *R.S.S Discovery* in the Celtic Sea, as part of the NERC funded Shelf Sea Biogeochemistry program in April 2015. In addition, a second LoC ΣNO_x sensor was mounted on a Conductivity-Temperature-Depth (CTD; Seabird 911 plus) rosette to enable direct comparison of its measurements to concentrations of ΣNO_x from seawater samples collected *in situ* at the same depth and time.

A single LoC $\sum NO_x$ sensor (Ocean Technology and Engineering Group, National Oceanography Centre, Southampton, UK) was integrated within the science bay of a Kongsberg Seaglider (Ogive fairing) and deployed from the *R.S.S Discovery* in the Celtic Sea, as part of the NERC funded Shelf Sea Biogeochemistry program in April 2015. In addition, a second LoC $\sum NO_x$ sensor was mounted on a Conductivity-Temperature-Depth (CTD; Seabird 911 plus) rosette to enable direct comparison of its measurements to concentrations of $\sum NO_x$ from seawater samples collected *in-situ* at the same depth and time in July 2015.

Both LoC deployments by Seaglider and discrete ship-based CTD rosette samples were collected from the Central Celtic Sea site (CCS; Fig. 1) located ~137

miles off the Cornish coast, UK (49°24.134'N, 8°36.248'W), with a water column depth of ~ 145 m. The Seaglider with integrated LoC $\sum NO_x$ sensor was deployed for 21 days (4th-25th April 2015) and completed 776 dives within 10 km of the CCS station. A total of 24 CTD casts within < 22 km of CCS were also conducted, allowing for comparison between discrete water samples and the LoC $\sum NO_x$ sensor. The rosette package consisted of a Seabird 911 plus CTD and 24 bottle Niskin system, which was used to collected discrete seawater samples. Chlorophyll *a (*hereafter Chl-*a*) was measured on a pre-calibrated (spinach extract, Sigma Aldrich) fluorometer (Turner Design Trilogy). Water samples collected from the Niskin bottles were analysed onboard for NO_3^-+$NO_{2,}^-$ using a segmented-flow autoanalyzer (Bran & Luebbe) following the colorimetric procedures of Woodward and Rees (2001).

The LoC ΣNO_x sensor is composed of a three-layer PMMA chip which contains precision-milled microchannels (150 µm wide, 300 µm deep), mixers and optical components consisting of LEDs (525 nm, Avago Technologies, USA) and photodiodes. Syringe pump, valves and electronics are mounted on the chip, which was encased in a mineral oil-filled housing (PVC, 12 cm diameter, 30 cm height) with an internally fitted pressure-compensating bladder. The LoC ΣNO_x sensor uses colourimetric detection, using the Griess assay (Grasshoff et al., 2009) where NO_3^- is reduced to NO_2^- using an off-chip copper activated cadmium column to enable ΣNO_x to be determined. A detection limit of 20 nM and linear range of up to 350 µM have been demonstrated in laboratory settings (Beaton et al., 2012). The LoC ΣNO_x sensor relies on a standard measurement and a blank measurement to determine the concentration of the sample. All reagents (Griess, imidazole buffer), standard and blank solutions were stored in externally attached gas impermeable 150 mL Flexboy bags (Sartorius, UK) and the waste was collected into a 500 ml Flexboy bag. The LoC ΣNO_x sensor, reagents and

126 standards used in this study have previously been described in detail by Beaton *et al.*,
127 (2012 & 2011) where it was deployed in a dynamic estuarine environment. More
128 recently, the LoC ΣNO_x sensor was deployed on a benthic lander in the Mauritian
129 oxygen minimum zone to examine cross-shelf transport of NO_3^- rich waters (Yücel et
130 al., 2015), and in glacial meltwaters rivers draining the Greenland Ice Sheet (Beaton et
131 al., 2017).

132 The LoC $\sum NO_x$ sensor was integrated into the payload bay of the Seaglider
133 (Fig. 2) and connected by cable directly into one of the glider serial ports. The inlet tube
134 with filter is located on the surface of the payload bay cover ~30 cm behind the CT sail
135 (Seabird Electronics). The Seaglider software uses a CNF file that contains the
136 configuration for each on-board instrument and a CMD file that provides mission
137 parameters. The CNF file enables communication between the Seaglider and the LoC
138 $\sum NO_x$ sensor. The LoC $\sum NO_x$ sensor is set to 'logger' in the CNF file, which enables
139 the glider to send a number of commands. These commands allow the Seaglider to send
140 and receive data to and from the sensor. Some of the key commands are 'clock-set',
141 used only at the start of each dive but enables the sensor to store any time offset between
142 glider and LoC $\sum NO_x$ sensor, 'status' which sends the sensor depth every 5 seconds
143 along with 3 trigger values and 'download' sent at the end of each dive requesting the
144 sensor to send both ascent and descent data files of processed $\sum NO_x$ values. During
145 deployments the CMD file is typically transmitted to the Seaglider by satellite and
146 includes three trigger values that can be passed to the LoC $\sum NO_x$ sensor using the
147 'status' command. These triggers are used to modify sensor behaviour at different
148 depths. Primarily these are used to ensure the LoC $\sum NO_x$ sensor does not take samples
149 on the surface and risk the intake of air, and to aid with additional blank and standard
150 measurements.

For deployments on the CTD rosette, the LoC ΣNO_x sensor was programmed in a continuous mode and performed a repeating measurement sequence of artificial seawater blank, sample, and NO_3^- standard (3 μM), until the CTD rosette was recovered to 5 m where the power was turned off. The operation of the LoC sensor was as follows; The seawater sample was drawn into the sensor through a 0.45μm MILLEX-HP filter unit (Millipore). Both the filtered seawater sample and imidazole buffer were pushed simultaneously through a serpentine mixer (used to aid mixing) before moving through an off-chip cadmium column. Griess reagent was added to the resultant buffered reduced seawater sample and then pushed through the 25mm absorption measurement cell, where the pink-coloured azo dye developed. Absorbance was calculated by comparing the optical intensity measured by the photodiode after a 100s reaction wait time for each measurement. Each step involved 7 flushes prior to the measurement to minimize sample carryover. Photodiode data was recorded at 1 Hz and the average of the last 10 readings of each wait stage was used to calculate absorbance, according to the Beer-Lambert law. Concentrations were calculated by comparing the absorbance of each sample to that of the subsequent standard measurement. This results in one blank-corrected sample measurement and standard every 17min during CTD deployments.

For the Seaglider deployments, the LoC ΣNO_x sensor was programmed to obtain a minimum of one artificial seawater blank and a standard measurement (6.5 μM NO_3^-) at the beginning and end of each dive. After the first measurement of blank and standard, continuous sample measurements took place on both the descent and ascent until the glider was at 10 m. Discrete seawater samples were drawn through a 0.45 μm MILLEX-HP filter unit (Millipore) into the sensor within the payload bay. Over the period of sampling (21 days) this resulted in 312 and 199 artificial seawater blanks and

standards, which was sufficient to determine both the ΣNO_x concentration and any drift associated with either the artificial seawater blank and/or the NO_3^- standard.

The Seaglider is a buoyancy driven autonomous underwater vehicle capable of multi-month deployments collecting high-resolution profiles of physical and biogeochemical parameters to 1000 m with a maximum travel range of 4,600 km (Rudnick et al., 2004). Bilateral communication between the Seaglider and base station, through an Iridium satellite connection, allowed dive configurations to be modified once deployed. Data was transmitted back to shore during deployments to assess the performance of the LoC ΣNO_x sensor. In addition to the LoC ΣNO_x sensor within the science bay, the Seaglider measured conductivity & temperature (non-pumped Sea-Bird SBE13 CT Sail, Seabird Electronics), pressure (Pain Electronics) and fluorescence, turbidity and optical backscatter (Triplet Ecopuck, Wet Labs). Conductivity, temperature and pressure were collected at a frequency of 1 Hz during deployment with all dive profiles lying within 4 km of CCS (Fig. 1). Temperature and conductivity were extracted and processed using the UEA Glider Toolbox (Queste, 2013). These routines apply manufacturer calibrations, correct for thermal inertia following the methods of Garau *et al.*, (2011) remove spikes and anomalous data, and draw upon a flight model similar to that described by Frajka-Williams *et al*., (2011). Four CTD casts, taken within 1.6 km of the glider, were used to calibrate the temperature and salinity. Manufacturer calibrations were initially applied to data from the Wetlabs Triplet for coloured dissolved organic matter (CDOM), backscatter & fluorescence by subtracting the instrument blank and applying a scaling factor. Calibration to convert fluorescence to Chl-*a* is based on the sensor's response to a cultured diatom, *Thalassiosira weissflogii* at a known Chl-*a* concentration (Hemsley et al., 2015; Sea-Bird Scientific, 2017).

3. Results and Discussion

The ability of the LoC $\sum NO_x$ sensor to accurately determine $\sum NO_x$ was assessed in two ways: (i) by comparison of the LoC $\sum NO_x$ sensor mounted on the stainless-steel rosette with discrete water samples collected using Niskin bottles at the same time and (ii) by comparing profiles obtained from the LoC $\sum NO_x$ sensor deployed within the glider with discrete water samples collected from the CTD on the same day at CCS. The LoC $\sum NO_x$ sensor, along with battery and reagents, was a similar size to the 20L Niskin bottle and was mounted in place of a single Niskin bottle on the frame. Once below 5 meters, a pressure sensor on the battery activated the power to the LoC $\sum NO_x$ sensor. The CTD rosette was held at three depths (45, 50 & 90 meters) for at least 90 minutes to allow for triplicate LoC $\sum NO_x$ sensor measurements at the prescribed depth, each bracketed by a blank and standard measurement. During this time period, two Niskin bottles were fired, one within 5 minutes of the first LoC $\sum NO_x$ sensor measurement and the second within 5 minutes of the last LoC $\sum NO_x$ sensor measurement. Water was collected from these discrete bottle firings for determination of $NO_3^-+NO_2^-$ concentrations using the segmented flow autoanalyzer in the ship-based laboratory. Figure 3a indicates the excellent agreement between sensor measurements and analysis of discrete water samples with a correlation of $r^2 = >0.99$ ($n = 9$; $p = <0.001$). The estimated analytical uncertainty of the LoC $\sum NO_x$ sensor was calculated from two times the standard deviation of the absorbance value of the deployed standard over the three deployments and was 0.14 µM ($n = 10$). This analytical uncertainty is higher than reported values for traditional segmented flow autoanalyzer analysis of $\sum NO_x$ (0.03-0.07 µM; Dafner, 2015) but lower than previous LoC $\sum NO_x$ deployments (0.4-1 µM; Yücel *et al.*, 2015).

LoC ΣNO_x data, collected from within the glider, was compared with NO_3^- + NO_2^- values from 24 CTD profiles collected at CCS throughout the 21 day deployment. Unlike the previous assessment of analytical uncertainty, data from the CTD profiles were not collected at the same time (1–10 h window) or depth range (± 3 m) and all samples were collected in a dynamic shelf sea system. Fig. 3b however, shows the excellent agreement the LOC ΣNO_x data and the discrete water sample measurements over the 21day period, with a correlation of $r^2 \geq 0.98$ ($n = 51$; $p \leq 0.001$). The average estimated analytical un- certainty for the LoC ΣNO_x sensor during this period was 0.19μM (n = 142) similar to the 0.14 μM (n = 10) for the CTD NO_3^- profiles.

Initial Seaglider dives (4^{th} to 9^{th} of April) were configured in a standard flight mode, whereby the Seaglider adjusts its pitch and buoyancy to maintain a uniform glide slope and descent and ascent speed (Eriksen et al., 2001). The LoC ΣNO_x sensor was switched on at the beginning of each dive and completed a blank and standard measurement followed by continuous measurements. The LoC ΣNOx sensor acquired depth information directly from the Seaglider, and using a depth trigger at 10 m the sensor recognized the Seaglider was diving and after completing its current blank or standard measurement would undertake continuous sample measurements. Triggers were also used to take advantage of extra time at the beginning, apogee and end of dives to undertake extra blank and standard measurements.

Fig. 4a shows that when the Seaglider was operated in the standard dive mode, the LoC ΣNO_x sensor carried out 5 sample measurements per 120 m dive with a total dive time of 30 ± 8 min. Moreover, these measurements were always in the same depth ranges within the water column due to the relatively shallow water column (~145m) and sensor operation timings. Fig. 4b shows the excellent agreement be- tween the LoC ΣNO_x sensor and traditional CTD segmented flow autoanlyzer measurements, for one

single CTD cast at 02:06 am and sixteen dives by the Seaglider from 00:18 to 09:25 am on the 6th of April 2015. However, the temporal and spatial resolution of ΣNO_x data (over the period of the day within the surface layer and across boundaries such as the nitricline) would not be sufficient to investigate the depletion of ΣNO_x as the spring bloom develops. As the glider can be controlled remotely, to increase the distribution of measurements by the LoC ΣNO_x sensor throughout the water column, (in particular across the nitricline), a second dive methodology - termed a 'loiter' dive - was employed. After the Seaglider has reached its maximum depth for that particular dive and started its ascent, for 30 mins the ascent angle was lowered and the glider 'loitered', thus increasing the resolution of measurements within the water column (Fig. 4a). Selected maximum target depths (90, 60, 40 and 25 m) were used to control the maximum dive depth and ensured a higher number of measurements in areas of interest (Fig. 4c). Loiter dives to 90 m doubled the amount of measurements made compared to the previous standard dives. Fig. 4c shows a comparison between ΣNO_x concentrations from two CTD casts at 02:06 and 08:22 am and LoC ΣNOx concentrations from seven 'loiter' dives from 11:19 am to 16:25 pm on the 15_{th} of April 2015. Once more, good agreement between the LoC ΣNO_x sensor and traditional segmented flow autoanlyzer measurements of CTD discrete samples was observed throughout the whole water column during this 14-h period. To ascertain the ability of the LoC ΣNO_x sensor to make comparable measurements to the segmented flow autoanlyzer, over an extended time period (4_{th} to 25_{th} April 2015), we compared the measurements within the bottom layer at 60–120 m where little changes in ΣNOx were observed. Excellent agreement between both the segmented flow autoanlyzer (6.86 ± 0.09 μM; n = 22) and LoC ΣNO_x sensor (6.86 ± 0.16 μM; n = 120) was observed. We have demonstrated the ΣNO_x concentrations measured from the LoC ΣNO_x sensor are com- parable to those of the

shipboard measurements analyzed on a segment flow autoanlyzer. Moreover, this shows that accurate measurements can be obtained from the LoC ΣNO_x wet chemical sensor over 21 days in a dynamic shelf environment.

On-board calibration with artificial seawater blanks and NO_3^- standard for each dive enables both the monitoring of instrument performance and stability over long-term deployments. To ensure maximum efficiency of the cadmium column, where NO_3^- is reduced to NO_2^- a flow rate of 150µl/min was chosen (Beaton et al., 2012). However, it is important to monitor any drift in the efficiency of the cadmium column over time as this may impact on the ΣNO_x concentrations. In this study, a decrease in absorbance values was observed, likely due to the gradual reduction in efficiency of the cadmium column over time. As sample concentrations are calculated from their associated blank and standard measurements, where the ratio of the absorbance of the sample and standard are determined, any drift caused by the decreasing reduction efficiency of the cadmium column is compensated for. Our results demonstrate that any decrease in absorbance values observed did not impact on the accurate determination of ΣNO_x from the LoC as shown by the excellent agreement with traditional autoanlyzer ΣNO_x method from discrete water samples collected throughout the 21-day deployment.

The data set presented here was collected during the spring phytoplankton bloom, a period during which integrated net productivity becomes greater than integrated losses and phytoplankton biomass accumulates in surface waters (Sverdrup, 1953). Over the 21-day deployment the LoC ΣNO_x sensor was able to accurately capture the large drawdown of ΣNO_x within the surface layer due to the onset of the spring bloom (Fig. 5). Concentrations decreased from 5.74 µM (4^{th}) to 1.42µM (25^{th}),

whilst bottom layer NO_3^- concentrations remained constant (6.86 ± 0.16 μM), as observed in previous studies within the Celtic Sea (Tweedle, 2007; Williams, 2013).

At the start of the deployment (4th – 6th April 2015), a small 0.8 μM difference between near surface (20–40 m) and bottom water (60-80 m) ΣNO_x concentrations was observed. During this time, surface Chl-a concentrations were relatively low (1.8 mg m^{-3}), but much higher (by 1.5 mg m^{-3}) than those typically observed during the winter in the area (Pingree et al., 1976; Smyth et al., 2010). This suggests that some phytoplankton growth had already occurred prior to deployment of the glider.

Between the 4th and 6th April the ΣNO_x concentration between 20 and 40 m remained constant. Any changes in the near surface (< 20 m) water however, where you might expect the largest drawdown in NO_3^-, were not resolved since the standard dive pattern used during this early period did not result in near surface LoC ΣNO_x measurements being made. Nevertheless, it is clear from Fig. 5 that a large drawdown of 3μM ΣNO_x occurred between the 4th and 11th of April 2015 (< 40 m) as stratification of the water column initialized. This can be backed up with the observed increase in surface water Chl-a, from 1.8 mg m^{-3} to 3.7 mg m^{-3}, indicative of phytoplankton growth, and thus nutrient drawdown, during the onset of the spring bloom. Changing the dive configuration to 'loiter' dives on the 11th of April in- creased the resolution of ΣNO_x surface data.

Just as the temperature sensor resolves the gradual deepening and warming of the surface mixed layer, the LoC ΣNO_x sensor resolves the coincident deepening of the nitricline and drawdown of ΣNOx above it. Between the 4th and 25th April surface waters warmed by > 1 °C and a 40 m deep thermocline is established. During this time

there is a 4.2 μM drawdown of ΣNO_x and an increase in Chl-a from a background of 1.8mg m^{-3} to4–6.8mg m^{-3}.

By the end of the Seaglider deployment (25th) a two-layer water column had developed with a warm, nutrient depleted, 40 m surface layer overlying colder, nutrient rich bottom waters. Previous studies suggest that phytoplankton growth starts to become ΣNO_x limited when concentrations fall below 1 μM (Eppley et al., 1969). The low surface water ΣNO_x concentrations (1.4 μM) measured during the end of the deployment suggest that this was close to happening. This is supported by a coinciding decrease in Chl-a (to < 2 mg m^{-3}) towards the end of the deployment. Ship-based observations show that it was not until the 28th that surface water concentration were below the limit of detection of 0.1 μM (Birchill et al., 2017).

This study has demonstrated for the first time that it is possible to accurately measure ΣNO_x over long-term deployments using a wet chemical nutrient sensor deployed within a glider. Our study provides a novel methodology, of differing operational characteristics to current high-resolution capable methodology (Johnson et al., 2013), enabling an increase in observations of ΣNO_x dynamics in temperate shelf seas during key transitional events (e.g. the onset of stratification and the spring bloom, convective overturning and the autumn bloom) and across fine-scale vertical and horizontal features (e.g. tidal mixing fronts, sub-surface chlorophyll maximum). At present, wet chemical biogeochemical sensors do not have the vertical resolution capabilities of the commonly used physical and optical sensors such as temperature, fluorescence or established ultraviolet spectrophotometer nitrate sensors (Johnson and Coletti, 2002). This resolution could be further improved by decreasing the time taken between measurements. By in- creasing flow rate, decreasing colour development time, decreasing the number of flushes and increasing N.E.D (naphthylethylenediamine di-

hydrochloride) concentration and reaction temperature, an increased measurement resolution could be achieved, but at the expense of measurement sensitivity (Beaton et al., 2012; Pai et al., 1990).

For long-term deployment of wet chemical sensors, reduced re- source consumption (power and reagents) and compact size are the main advantages of microfluidic systems. Deployment of sensors on moorings, where solar and wind power are available, negates power constraints. However, for autonomous underwater vehicles power be- comes the greatest limiting resource (Dickey et al., 2008). During the 21-day deployment, the LoC ΣNO_x sensor (version 3.2) had a low power consumption of 1.5 W. This was only marginally higher than the other standard sensor packages on the Seaglider (0.9 W and 0.25 W for the Wetlabs ECO Triplet and SBE pumped payload CTD respectively), but lower than other wet chemical and UV absorption systems (e.g. ISUS V3, Satlantic, USA; NitraVis, YSI, USA; SubChemPak, SubChem Systems, USA). A single dive of the LoC ΣNO_x sensor consumed 2.5 mL of Griess reagent, 2.5 mL of buffer solution and 0.21 mL of standard and blank solution achieving 1 blank and standard measurement and ~ 10 samples on a dive to 120 m. This would enable a total of 400 dives to be made and 4000 sample measurements. During this study, the LoC was only active during periods when the R.S.S Discovery was also sampling at CCS to enable a direct comparison between the two types of measurements over a long-term deployment of the LoC. This resulted in accurate LoC ΣNO_x determined over 21 days. With a sampling strategy focused on achieving the maximum amount of measurements, a profile consisting of 10 sample measurements could be undertaken every ~ 40 min, allowing for increased observations of episodic and transient events unable to be observed by discrete sampling.

4. Conclusion

The temporal and spatial variability of biogeochemical processes has been successfully measured through the use of remote sensing, time series moorings and ship-based methods, but these, to an extent, fall short in resolving the dynamic temporal and spatial elements with long- term endurance in a low cost package. From this, there has been a strong call for the development of biogeochemical sensors to be deployed, on stationary and mobile platforms, to provide in situ measurements as part of sensor networks aimed at providing long term monitoring within a low cost package (Adornato et al., 2010; Johnson et al., 2009). The LoC ΣNO_x sensor deployed within the Seaglider in this study clearly demonstrates that nitrate & nitrite can be accurately determined over monthly timescales due to the sensor's low resource use, small size and in situ calibration abilities. Moreover, deployed within a glider with other physical and biochemical data (e.g. CTD and the Wetlabs Triplet sensor measurements), it provided a powerful tool for resolving dynamic biogeochemical processes within a dynamic shelf system.

Acknowledgements

The authors would like to thank the captain and crew of the RSS Discovery. This project was funded by UK Natural Environmental Research Council through the Sensors on Gliders program (NE/J020184/1) to MCL and (NE/K001701/1) to JEH. The field deployment took place under the Shelf Sea Biogeochemistry program with funding to MCL from NERC (NE/K001779/1). Funding from the European Union Seventh Framework Program (FP7/2007-2013) under grant agreement n°614141 (SenseOCEAN) contributed to the research leading to these results. We would also like to thank David White, Alvaro Lorenzo Lopez, Sam Ward, James Burris and Stephen

398 Woodward of the Marine Autonomous and Robotics Systems group, and David
399 Owsianka and Adrian Nightingale of the Ocean Technology and Engineering group at
400 the National Oceanography Centre, UK.
401

References

Adornato, L., Cardenas-Valencia, A., Kaltenbacher, E., Byrne, R., Daly, K., Larkin, K., Hartman, S., Mowlem, M., Prien, R., Garcon, V., 2010. In Situ Nutrient Sensors for Ocean Observing Systems, in: Hall, J., Harrison, D.E., Stammer, D. (Eds.), Proceedings of OceanObs'09: Sustained Ocean Observations and Information for Society. European Space Agencey, pp. 9–18. https://doi.org/10.5270/OceanObs09.cwp.01

Beaton, A.D., Cardwell, C.L., Thomas, R.S., Sieben, V.J., Legiret, F.-E., Waugh, E.M., Statham, P.J., Mowlem, M.C., Morgan, H., 2012. Lab-on-chip measurement of nitrate and nitrite for in situ analysis of natural waters. Environ. Sci. Technol. 46, 9548–56. https://doi.org/10.1021/es300419u

Beaton, A.D., Sieben, V.J., Floquet, C.F. a., Waugh, E.M., Abi Kaed Bey, S., Ogilvie, I.R.G., Mowlem, M.C., Morgan, H., 2011. An automated microfluidic colourimetric sensor applied in situ to determine nitrite concentration. Sensors Actuators B Chem. 156, 1009–1014. https://doi.org/10.1016/j.snb.2011.02.042

Beaton, A.D., Wadham, J.L., Hawkings, J., Bagshaw, E.A., Lamarche-Gagnon, G., Mowlem, M.C., Tranter, M., 2017. High-Resolution in Situ Measurement of Nitrate in Runoff from the Greenland Ice Sheet. Environ. Sci. Technol. 12518–12527. https://doi.org/10.1021/acs.est.7b03121

Birchill, A.J., Milne, A., S. Woodward, E.M., Harris, C., Annett, A., Rusiecka, D., Achterberg, E.P., Gledhill, M., Ussher, S.J., Worsfold, P.J., Geibert, W., Lohan, M.C., 2017. Seasonal iron depletion in temperate shelf seas. Geophys. Res. Lett. 8987–8996. https://doi.org/10.1002/2017GL073881

425 Dafner, E. V., 2015. Segmented continuous-flow analyses of nutrient in seawater:
426 Intralaboratory comparison of Technicon AutoAnalyzer II and Bran+Luebbe
427 Continuous Flow AutoAnalyzer III. Limnol. Oceanogr. Methods 13, 511–520.
428 https://doi.org/10.1002/lom3.10035

429 Davidson, K., Gilpin, L.C., Pete, R., Brennan, D., McNeill, S., Moschonas, G.,
430 Sharples, J., 2013. Phytoplankton and bacterial distribution and productivity on
431 and around Jones Bank in the Celtic Sea. Prog. Oceanogr. 117, 48–63.
432 https://doi.org/10.1016/j.pocean.2013.04.001

433 Dickey, T.D., Itsweire, E.C., Moline, M., Perry, M.J., 2008. Introduction to the
434 Limnology and Oceanography Special Issue on Autonomous and Lagrangian
435 Platforms and Sensors (ALPS). Limnol. Oceanogr. 53, 2057–2061.
436 https://doi.org/10.4319/lo.2008.53.5_part_2.2057

437 Eppley, R.W., Rogers, J.N., Mccarthy, J.J., 1969. for Uptake of Nitrate and
438 Ammonium. Methods.

439 Eriksen, C.C., Osse, T.J., Light, R.D., Wen, T., Lehman, T.W., Sabin, P.L., Ballard,
440 J.W., Chiodi, A.M., 2001. Seaglider: A long-range autonomous underwater
441 vehicle for oceanographic research. IEEE J. Ocean. Eng. 26, 424–436.
442 https://doi.org/10.1109/48.972073

443 Fasham, M.J.R., Holligan, P.M., Pugh, P.R., 1983. The Spatial and Temporal
444 Development of the Spring Phytoplankton Bloom in the Celtic Sea , April 1979.
445 Prog. Oceanogr. 12, 87–145. https://doi.org/10.1016/0079-6611(83)90007-1

446 Frajka-Williams, E., Eriksen, C.C., Rhines, P.B., Harcourt, R.R., 2011. Determining
447 vertical water velocities from Seaglider. J. Atmos. Ocean. Technol. 28, 1641–

1656. https://doi.org/10.1175/2011JTECHO830.1

Garau, B., Ruiz, S., Zhang, W.G., Pascual, A., Heslop, E., Kerfoot, J., Tintoré, J., 2011. Thermal lag correction on slocum CTD glider data. J. Atmos. Ocean. Technol. 28, 1065–1071. https://doi.org/10.1175/JTECH-D-10-05030.1

Grasshoff, K., Kremling, K., Ehrhardt, M. (Eds.), 2009. Mehtods of seawater analysis. John Wiley & Sons.

Hemsley, V.S., Smyth, T.J., Martin, A.P., Frajka-Williams, E., Thompson, A.F., Damerell, G., Painter, S.C., 2015. Estimating Oceanic Primary Production Using Vertical Irradiance and Chlorophyll Profiles from Ocean Gliders in the North Atlantic. Environ. Sci. Technol. 49, 11612–11621. https://doi.org/10.1021/acs.est.5b00608

Hickman, A., Moore, C., Sharples, J., Lucas, M., Tilstone, G., Krivtsov, V., Holligan, P., 2012. Primary production and nitrate uptake within the seasonal thermocline of a stratified shelf sea. Mar. Ecol. Prog. Ser. 463, 39–57. https://doi.org/10.3354/meps09836

Hickman, A.E., Holligan, P.M., Moore, C.M., Sharples, J., Krivtsov, V., Palmer, M.R., 2009. Distribution and chromatic adaptation of phytoplankton within a shelf sea thermocline. Limnol. Oceanogr. 54, 525–536.

Johnson, K., Berelson, W., Boss, E., Chase, Z., Claustre, H., Emerson, S., Gruber, N., Körtzinger, A., Perry, M.J., Riser, S., 2009. Observing Biogeochemical Cycles at Global Scales with Profiling Floats and Gliders: Prospects for a Global Array. Oceanography 22, 216–225. https://doi.org/10.5670/oceanog.2009.81

Johnson, K.S., Coletti, L.J., Jannasch, H.W., Sakamoto, C.M., Swift, D.D., Riser, S.C.,

2013. Long-Term Nitrate Measurements in the Ocean Using the in situ Ultraviolet Spectrophotometer: Sensor Integration into the APEX Profiling Float. J. Atmos. Ocean. Technol. 30, 1854–1866. https://doi.org/10.1175/JTECH-D-12-00221.1

Nightingale, A.M., Beaton, A.D., Mowlem, M.C., 2015. Trends in Microfluidic Systems for In Situ Chemical Analysis of Natural Waters. Sensors Actuators B Chem. 221, 1398–1405. https://doi.org/10.1016/j.snb.2015.07.091

Pai, S.C., Yang, C.C., P. Riley, J., 1990. Formation kinetics of the pink azo dye in the determination of nitrite in natural waters. Anal. Chim. Acta 232, 345–349. https://doi.org/10.1016/S0003-2670(00)81252-0

Palmer, M.R., Rippeth, T.P., Simpson, J.H., 2008. An investigation of internal mixing in a seasonally stratified shelf sea. J. Geophys. Res. 113, C12005. https://doi.org/10.1029/2007JC004531

Pingree, R.D., Holligan, P.M., Mardell, G.T., Head, R.N., 1976. The influence of physical stability on spring, summer and autumn phytoplankton blooms in the Celtic Sea. J. Mar. Biol. Assoc. United Kingdom 56, 845–873. https://doi.org/10.1017/S0025315400020919

Prien, R.D., 2007. The future of chemical in situ sensors. Mar. Chem. 107, 422–432. https://doi.org/10.1016/j.marchem.2007.01.014

Queste, B.Y., 2013. Hydrographic Observations of Oxygen and Related Physical Variables in the North Sea and Western Ross Sea Polynya. University of East Anglia.

Rippeth, T.P., 2005. Thermocline mixing in summer stratified continental shelf seas. Geophys. Res. Lett. 32, L05602. https://doi.org/10.1029/2004GL022104

494 Rippeth, T.P., Wiles, P., Palmer, M.R., Sharples, J., Tweddle, J., 2009. The diapcynal
495 nutrient flux and shear-induced diapcynal mixing in the seasonally stratified
496 western Irish Sea. Cont. Shelf Res. 29, 1580–1587.
497 https://doi.org/10.1016/j.csr.2009.04.009

498 Rudnick, D.L., 2016. Ocean Research Enabled by Underwater Gliders. Ann. Rev. Mar.
499 Sci. 8, 519–541. https://doi.org/10.1146/annurev-marine-122414-033913

500 Rudnick, D.L., Davis, R.E., Eriksen, C.C., Fratantoni, D.M., Perry, M.J., 2004.
501 Underwater Gliders for Ocean Research. Mar. Technol. Soc. J. 38, 73–84.

502 Sea-Bird Scientific, 2017. User manual ECO Fluorometers and Scattering Sensors
503 [WWW Document]. URL http://www.seabird.com/eco-triplet-fluorometer-and-
504 backscattering-sensor (accessed 10.25.17).

505 Sharples, J., Moore, M.C., Rippeth, T.P., Holligan, P.M., Hydes, D.J., Fisher, N.R.,
506 Simpson, J.H., Moore, C.M., Rippeth, T.P., Holligan, P.M., Hydes, D.J., Fisher,
507 N.R., Simpson, J.H., 2001. Phytoplankton distribution and survival in the
508 thermocline. Limnol. Oceanogr. 46, 486–496.
509 https://doi.org/10.4319/lo.2001.46.3.0486

510 Sharples, J., Tweddle, J.F., Green, J.A.M., Palmer, M.R., Kim, Y., Hickman, A.E.,
511 Holligan, P.M., Moore, C.M., Rippeth, T.P., Simpson, J.H., Krivtsov, V., 2007.
512 Spring – neap modulation of internal tide mixing and vertical nitrate fluxes at a
513 shelf edge in summer. Limnol. Oceanogr. 52, 1735–1747.

514 Simpson, J.H., Sharples, J., 2012. Introduction to the Physical and Biological
515 Oceanography of Shelf Seas. Cambridge University Press.
516 https://doi.org/10.1017/CBO9781139034098

Smyth, T.J., Fishwick, J.R., Al-Moosawi, L., Cummings, D.G., Harris, C., Kitidis, V., Rees, A., Martinez-Vicente, V., Woodward, E.M.S., 2010. A broad spatio-temporal view of the Western English Channel observatory. J. Plankton Res. 32, 585–601. https://doi.org/10.1093/plankt/fbp128

Sverdrup, H.U., 1952. On Conditions for the Vernal Blooming of Phytoplankton 18–287.

Takahashi, T., Sutherland, S.C., Wanninkhof, R., Sweeney, C., Feely, R.A., Chipman, D.W., Hales, B., Friederich, G., Chavez, F., Sabine, C., Watson, A., Bakker, D.C.E., Schuster, U., Metzl, N., Yoshikawa-Inoue, H., Ishii, M., Midorikawa, T., Nojiri, Y., Körtzinger, A., Steinhoff, T., Hoppema, M., Olafsson, J., Arnarson, T.S., Tilbrook, B., Johannessen, T., Olsen, A., Bellerby, R., Wong, C.S., Delille, B., Bates, N.R., de Baar, H.J.W., 2009. Climatological mean and decadal change in surface ocean pCO2, and net sea-air CO2 flux over the global oceans. Deep. Res. Part II Top. Stud. Oceanogr. 56, 554–577. https://doi.org/10.1016/j.dsr2.2008.12.009

Thomas, H., Bozec, Y., Elkalay, K., de Baar, H.J.W., 2004. Enhanced open ocean storage of CO2 from shelf sea pumping. Science 304, 1005–8. https://doi.org/10.1126/science.1095491

Tsunogai, S., Watanabe, S., Sato, T., 1999. Is there a “continental shelf pump” for the absorption of atmospheric CO2? Tellus, Ser. B Chem. Phys. Meteorol. 51, 701–712. https://doi.org/10.3402/tellusb.v51i3.16468

Tweddle, J.F., Sharples, J., Palmer, M.R., Davidson, K., McNeill, S., 2013. Enhanced nutrient fluxes at the shelf sea seasonal thermocline caused by stratified flow over

a bank. Prog. Oceanogr. 117, 37–47. https://doi.org/10.1016/j.pocean.2013.06.018

Tweedle, J., 2007. Nutrient Fluxes into the seasonal thermocline of the Celtic sea. University of Southampton.

Williams, C., 2013. The Supply of Nutrients To the Subsurface Chlorophyll Maximum in Temperate Shelf Seas.

Williams, C., Sharples, J., Mahaffey, C., Rippeth, T., 2013. Wind-driven nutrient pulses to the subsurface chlorophyll maximum in seasonally stratified shelf seas. Geophys. Res. Lett. 40, 5467–5472. https://doi.org/10.1002/2013GL058171

Woodward, E.M.S., Rees, A.P., 2001. Nutrient distributions in an anticyclonic eddy in the northeast Atlantic ocean, with reference to nanomolar ammonium concentrations. Deep. Res. Part II Top. Stud. Oceanogr. 48, 775–793. https://doi.org/10.1016/S0967-0645(00)00097-7

Yücel, M., Beaton, A.D., Dengler, M., Mowlem, M.C., Sohl, F., Sommer, S., 2015. Nitrate and Nitrite Variability at the Seafloor of an Oxygen Minimum Zone Revealed by a Novel Microfluidic In-Situ Chemical Sensor. PLoS One 10, 1–16. https://doi.org/10.1371/journal.pone.0132785

Figures

Captions

Figure 1. (a) Location of the Central Celtic Sea (CCS) sampling site (black cross) and shelf and shelf edge bathymetry. (b) Location of the Celtic sea on the North West European Shelf. (c) Seaglider tracks (black lines) and surfacing points (colour dots) in relation to CCS from the 4th to 25th of April 2015.

Figure 2. (a) Diagram of the locations of sensors deployed on the Seaglider (Kongsberg; Not to scale): (1) CT sail, (2) LoC, and (3) EcoPuck. (b) A LoC ∑NOx Sensor deployed with housing within the sensor payload bay of a Seaglider (Ogive Profile). (c) A LoC ∑NOx sensor consisting of (1) microfluidic chip, (2) custom electronics, and (3) syringe pump assembly.

Figure 3. Comparison of autoanalyzer (AA) and LoC $\sum NO_x$ measurements. (a) AA and *in situ* LoC $\sum NO_x$ measurements obtained from CTD casts. (b) AA and LoC $\sum NO_x$ measurements obtained from separate CTD casts (3rd to 6th, 11th, 12th, 15th, 16th, 20th, 21st and 25th) and *in situ* LoC glider profiles at CCS.

Figure 4. (a) Comparison of the two different dives used in this study. Blue and red diamonds indicate where $\sum NO_x$ measurements were obtained. (b) ∑NOx measurements from one CTD cast (02:06 am; dashed line) and sixteen standard dives (00:18 to 09:25 am; diamonds) from the 6th April 2015. (c) $\sum NO_x$ measurements from two CTD cast (02:06 and 08:22 am; dashed lines) and seven 'loiter' dives (11:19 to 16:25 pm; diamonds) from the 16th April 2015.

Figure 5. (a) temperature (˚C), (b) LoC $\sum NO_z$ (µM) and (c) mean surface (< 20 m) Chlorophyll-*a* measurements obtained from one Seaglider deployment from the

582 4th to 25th April 2015.

583
584
585
586
587
588
589
590
591

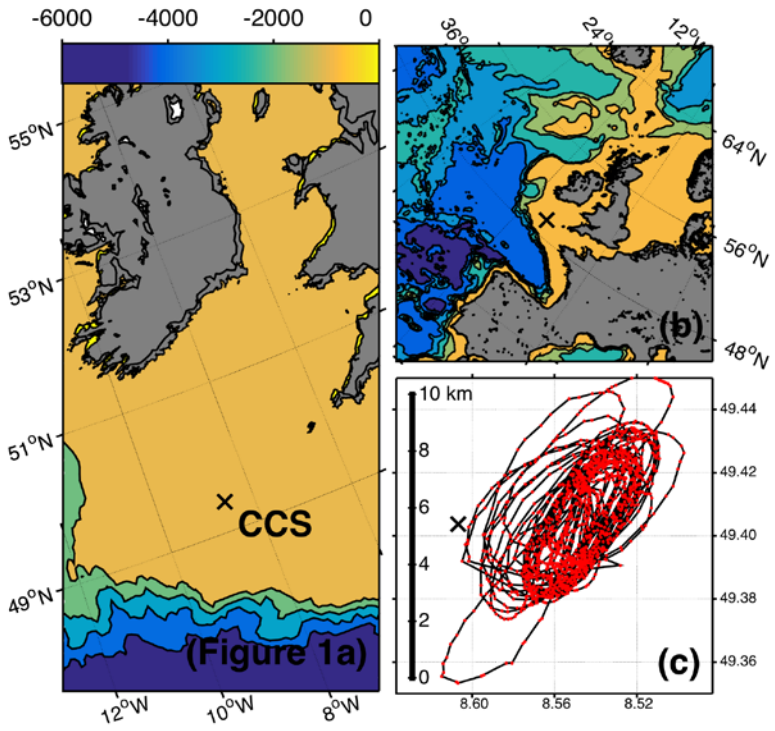

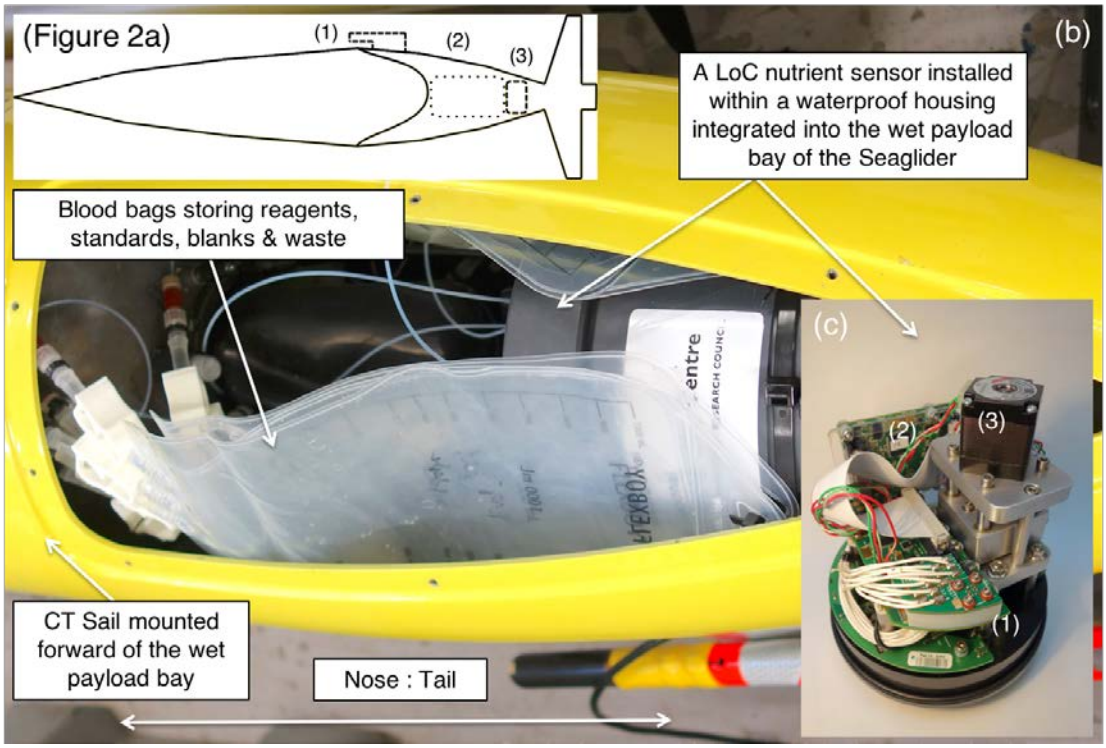

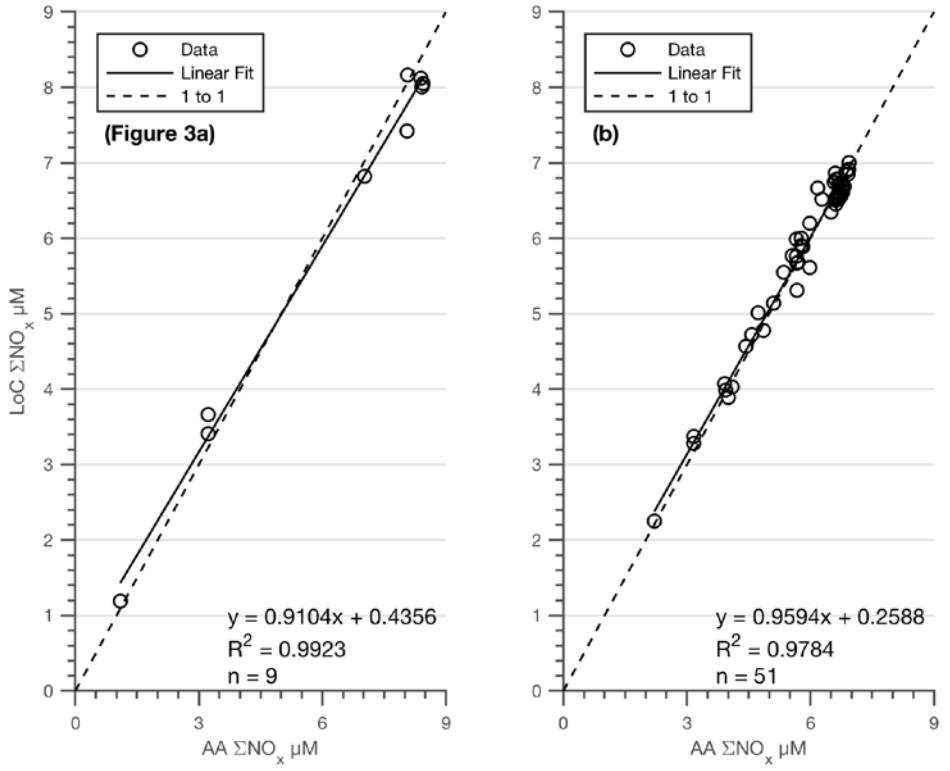
Data
Linear Fit
1 to 1
(Figure 3a)
y = 0.9104x + 0.4356
R2 = 0.9923
n = 9
LoC ΣNOx µM
AA ΣNOx µM
(b)
y = 0.9594x + 0.2588
R2 = 0.9784
n = 51

592

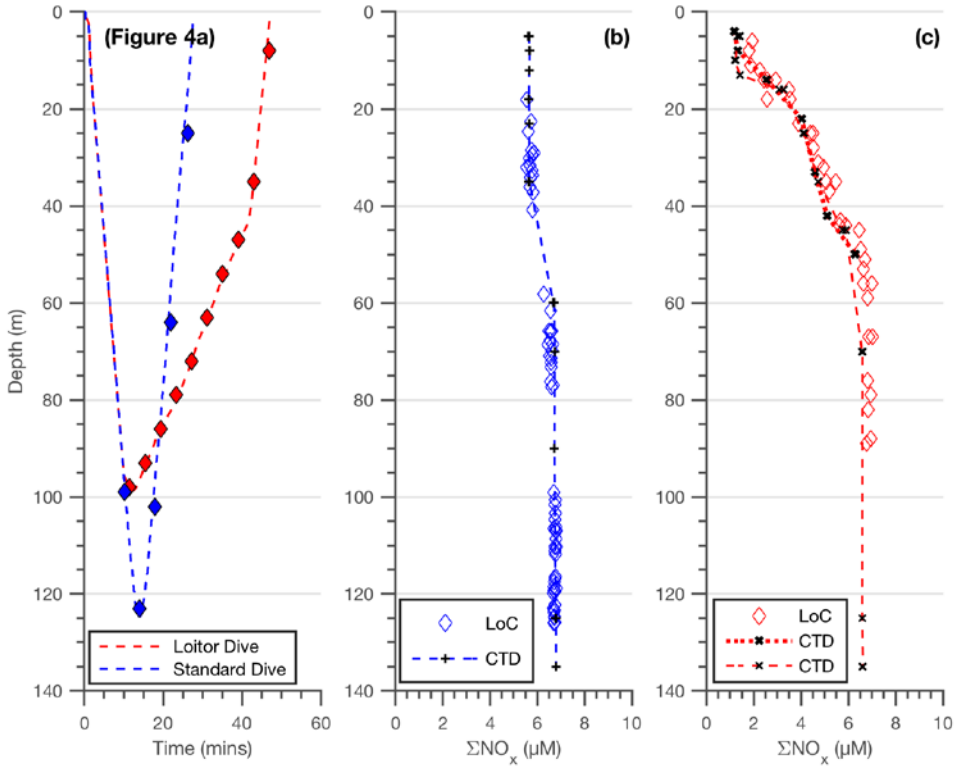
(Figure 4a)
Loitor Dive
Standard Dive
Depth (m)
Time (mins)
(b)
LoC
CTD
ΣNOx (µM)
(c)
LoC
CTD
CTD

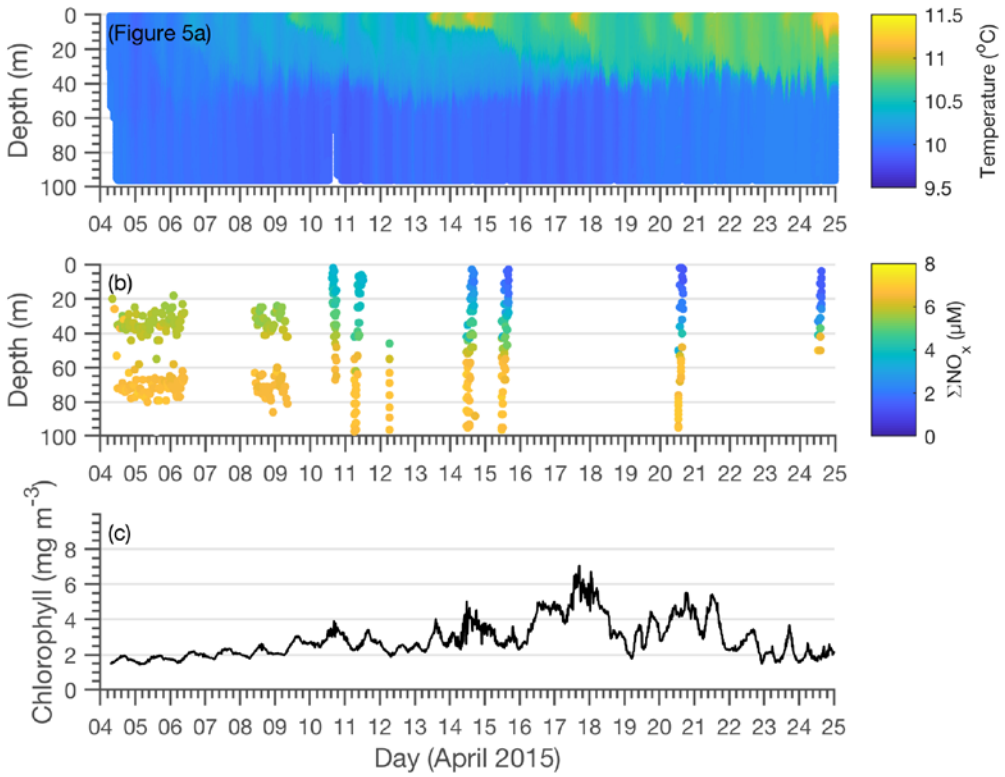
(Figure 5a)
Depth (m)
0
20
40
60
80
100
04 05 06 07 08 09 10 11 12 13 14 15 16 17 18 19 20 21 22 23 24 25
11.5
11
10.5
10
9.5
Temperature (°C)
(b)
Depth (m)
8
6
4
2
0
ΣNOx (μM)
(c)
Chlorophyll (mg m-3)
Day (April 2015)

593